

Pupil Shape Description Using Fourier Series

Soumyadip Rakshit and Donald M. Monro
Department of Electronic and Electrical Engineering,
University of Bath, Claverton Down,
Bath, BA2 7AY, United Kingdom.
{S.Rakshit, D.M.Monro}@bath.ac.uk

Abstract—In this work, improved performance is obtained in human iris matching systems using a Fourier-based description to approximate non-circular pupil boundaries in human eyes. The study also leads an analysis of pupil shape. Excellent fitting is obtained for non-ideal cases such as oblong, irregular, off-centre and dilated pupils, and improved iris normalization is obtained compared to best fit circles. The method is applied to 1912 eye images of 478 eyes from the Bath database and the effect of increasing the number of Fourier coefficients on the pupil outline accuracy is studied. The RMS pixel error between the outline and actual edge points is seen to decrease from 1.48 (for circles) to 0.34 (for 9 coefficients). Only 21 cases are found to produce low deviations from a circular boundary, indicating that a majority of pupils (98.9%) are non-circular. The Equal Error Rate (EER) in verification using the new method is estimated to be significantly reduced, at 7.5×10^{-5} compared to 1.2×10^{-4} for pupils fitted as circular.

Keywords—Biometrics, Iris, Image segmentation

Topic area—Biometrics.

I. INTRODUCTION

As security becomes an issue of paramount importance, biometrics [1] and iris recognition in particular have become subject of great interest. The human iris is a thin circular diaphragm lying between the cornea and the lens, and has a fine structure with many interlacing minute characteristics such as furrows, freckles, crypts and coronas. For every subject these characteristics are unique as a result of the individual differences that arise during embryonic development. Apart from general textural appearance and color, the detailed structure of an iris is not genetically determined but develops by a random process [2].

The iris is essentially stable over a person's lifetime and is ideal for non-invasive identification, being an externally visible internal organ. Pioneering work in this field was done by Daugman in the early nineties using Gabor wavelets [3, 4]. Although some research into non-circular localization has been done [5, 6], much work has been based on the assumption of pupil circularity, which as we will show is rarely the case. Additionally, even circular pupils appear oblong when viewed from an angle. In order to

address these issues and achieve good localization results, one needs to find exact pupil boundary points and describe an appropriate shape to connect them. In this paper we propose a Fourier based method which achieves this goal.

The paper is subdivided as follows. Section 2 presents a basic overview of segmenting the iris from an eye image. The mathematical background of the proposed method along with effects of higher coefficients on pupil outline is detailed in Section 3. Evaluations are described and conclusions drawn in Sections 4 and 5 respectively.

II. PREPROCESSING

This work assumes that a useful number of points can be found on the pupil boundary, which are not necessarily equally spaced. To do this, an approximate pupil location is first determined by searching for a dark area of significant size close to the image centre. A histogram analysis is then carried out to find a more exact centre and the average pupil radius. This approximate circular pupil boundary is then examined in detail to obtain 16 edge points. Points affected by specular reflections and eyelid/eyelash obfuscation are removed, and the remaining ones are connected using the Fourier-based shape description. The iris outline is modelled using connected semi-circular arcs, and the irregular annulus within these two boundaries is mapped onto a 512 x 80 pixel image. For matching, the 48 rows nearest the pupil are used to mitigate the effects of eyelids and eyelashes. The image is then intensity normalized by histogram stretching and compensated for variations in lighting. Fig. 1 shows typical stages in localization and normalization.

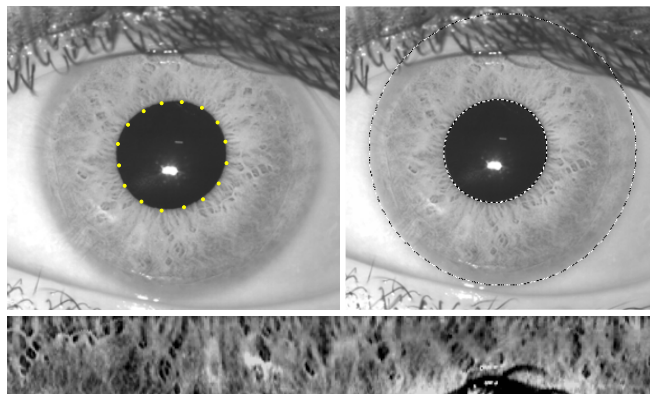


Fig. 1. Illustrating basic localization and normalization steps: Points on the actual pupil outline; Final pupil and iris boundaries; Unwrapped normalized rectangular iris 512 x 48 image.

III. PROPOSED FFT-BASED SHAPE DESCRIPTION

We wish to describe the distance $d(\theta)$ of a curve in the plane from a known or assumed centre as a harmonic function of the angle θ in the form of a 1D Fourier Series. It must be noted here that we are assuming the function $d(\theta)$ to be single valued in θ .

$$d(\theta) = \sum_{n=0}^N a_n \cos(n\theta) + b_n \sin(n\theta)$$

A standard Discrete Fourier Series (DFT) is a least squares fit of regularly spaced data and because of the orthogonality of the functions \cos and \sin results in the well DFT formula. However if the points given to fit, $\{r_i, \theta_i, i = 1 \dots M\}$ are irregular in θ , then the error in the fit is given by,

$$\begin{aligned} E(\theta_i) &= \sum_{i=1}^M (d(\theta_i) - r_i) \\ E^2 &= \sum_{i=1}^M E(\theta_i)^2 = \sum_{i=1}^M (d(\theta_i) - r_i)^2 \\ &= \sum_{i=1}^M \left[\sum_{n=0}^N a_n \cos n\theta_i + b_n \sin n\theta_i - r_i \right]^2 \end{aligned}$$

Thus, we wish to find $\{a_n, b_n; n = 0 \dots N\}$ such that the sum of squares of the error is minimized. To do this we differentiate the above with respect to a_k and b_k and equate to zero as follows,

$$\begin{aligned} \frac{\partial E^2}{\partial a_k} &= \sum_{i=1}^M 2 \left[\sum_{n=0}^N a_n \cos n\theta_i + b_n \sin n\theta_i - r_i \right] \cos k\theta_i = 0 \\ \frac{\partial E^2}{\partial b_k} &= \sum_{i=1}^M 2 \left[\sum_{n=0}^N a_n \cos n\theta_i + b_n \sin n\theta_i - r_i \right] \sin k\theta_i = 0 \end{aligned}$$

Noting that $b_0 = 0$, this can be expressed as the system of linear equations: $PV=C$; where the unknowns are V :

$$V = \begin{bmatrix} a_0 \\ a_1 \\ \vdots \\ a_N \\ b_1 \\ \vdots \\ b_N \end{bmatrix} \quad \text{and the right hand side is } C = \begin{bmatrix} C_0 \\ C_1 \\ \vdots \\ C_N \\ C_{N+1} \\ \vdots \\ C_{2N} \end{bmatrix}$$

$$\text{with } C_0 = \sum_{i=0}^M r_i, C_k = \sum_{i=0}^M r_i \cos k\theta_i \text{ and}$$

$$C_{N+k} = \sum_{i=0}^M r_i \sin k\theta_i \text{ for } k = 1 \dots N$$

The $2N + 1$ by $2N + 1$ matrix P , for all $k = 1 \dots N$ and $n = 1 \dots N$, is thus given by:

$$[\text{Upper Left Matrix}]: P_{k,n} = \sum_{i=1}^M \cos n\theta_i \cos k\theta_i$$

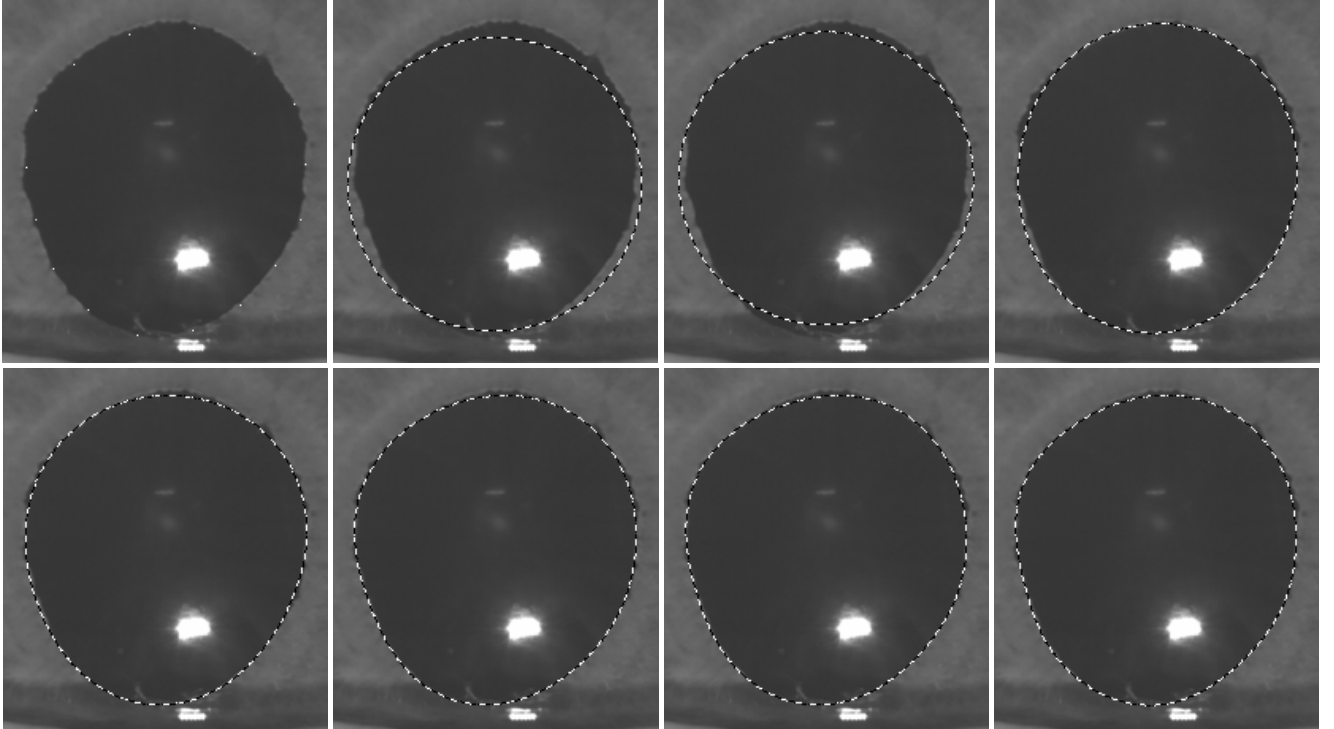


Fig. 2. Starting from top left: An irregular pupil with some actual pupil boundary points; best fit circular boundary; boundaries obtained using 3; 5; 7; 9; 11 and 13 Fourier series coefficients.

$$\text{[Upper Right Matrix]: } P_{k,N+n} = \sum_{i=1}^M \sin n\theta_i \cos k\theta_i$$

$$\text{[Lower Left Matrix]: } P_{N+k,n} = \sum_{i=1}^M \cos n\theta_i \sin k\theta_i$$

$$\text{[Lower Right Matrix]: } P_{N+k,N+n} = \sum_{i=1}^M \sin n\theta_i \sin k\theta_i$$

This matrix is symmetric and can be solved for any M and N giving an approximation by N harmonics to M given points. In the case where $M=N$ and the points are equally spaced in $\{\theta_i = 0, 2\pi/(N+1), \dots, 2N\pi/(N+1)\}$, the matrix P is diagonal and the solution is exactly the DFT. As the number of Fourier coefficients is increased, the resultant outline gets closer to the actual points. This effect is well illustrated in Fig. 2 for a highly irregular pupil. Starting from the top left, Fig. 2. shows 16 points on the boundary of a highly irregular pupil; best fit circular boundary; boundaries obtained using 3($a_0 a_1 b_1$); 5($a_0 a_1 b_1 a_2 b_2$); 7; 9 and 11 Fourier series coefficients. It may be noted that in the absence of enough accurate points on the pupil edge, the use of a high number of coefficients will lead to erroneous outlines. In general, the number of coefficients used should be limited to less than the number of actual points found on the pupil outline. Otherwise, the solution is a least square fit which forces the outline close to the given points at the expense of large oscillations in between; akin to the Gibbs phenomenon observed with the Fourier Series. Normalization results with circular and shape description localizations are shown in Fig. 3. While portions of the black pupil are visible in circular case, no such errors are seen in the latter one.

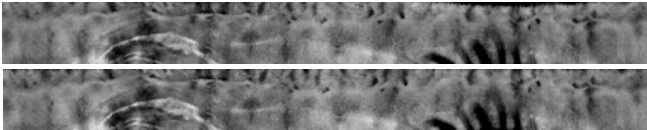


Fig. 3. Same iris image normalized using circular localization and 5-coefficient shape description.

IV. RESULTS

For evaluation, 1912 images of 478 eyes were used from the Bath database [7]. For each, the shape was fitted using between 1 and 9 Fourier series coefficients in steps of 2, where 1 corresponds to the best fit circle using only coefficient a_0 . The mean distance in pixels between the exact pupil edge points and the nearest ones on the outline were calculated. Figure 4 shows histograms of the numbers of pupils with particular levels of error as the number of coefficients is increased. The distribution clearly shifts towards smaller errors as the order of approximation increases. It is observed that very few pupils (21 out of 1912) lie in the lowest error bin of the circular localization histogram. From this it is seen that 99.8% of the pupils

analyzed have RMS errors greater than 0.75 pixels, some significantly greater. The change in RMS error averaged across all images is shown in Fig. 5. for the range of coefficients studied, and again shows clearly that the approximation error is reduced as the number of coefficients is increased.

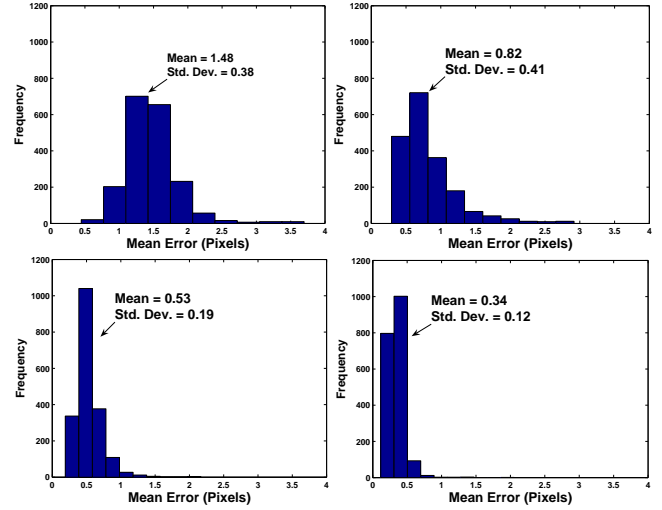


Fig. 4. Histograms illustrating the effect of increasing the number of coefficients on the error between actual points and described outline for (a) 1 – Best fit circle; (b) 3; (c) 5; and (d) 9 coefficients.

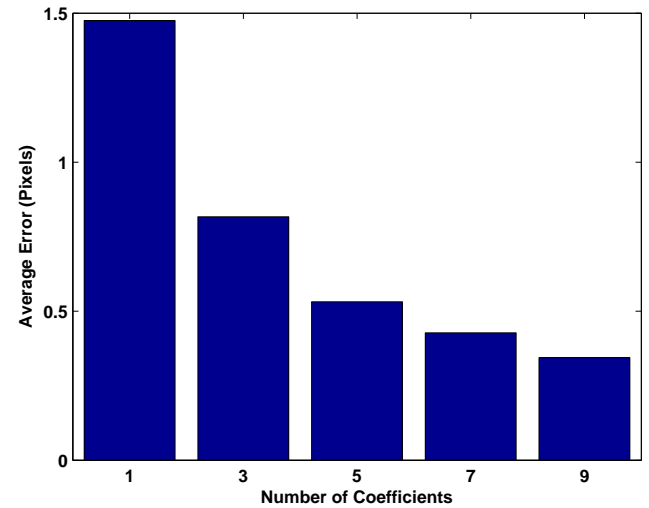


Fig. 5. Illustrating the decrease in RMS error between actual points and fitted outline with increased number of coefficients.

As a second experiment, 1784 normalized images from 446 eyes were selected for feature extraction and matching. For each eye, one image was used to enrol while the rest were used for testing. Coding was carried out using an in-house iris feature extraction method [8] and every test feature was compared against the whole database of enrolled ones. The comparison resulting in the lowest Hamming Distance (HD) was chosen as the matching iris. 100% Correct Recognition Rates were obtained on the entire dataset for all coefficients studied with no FAR or FRR.

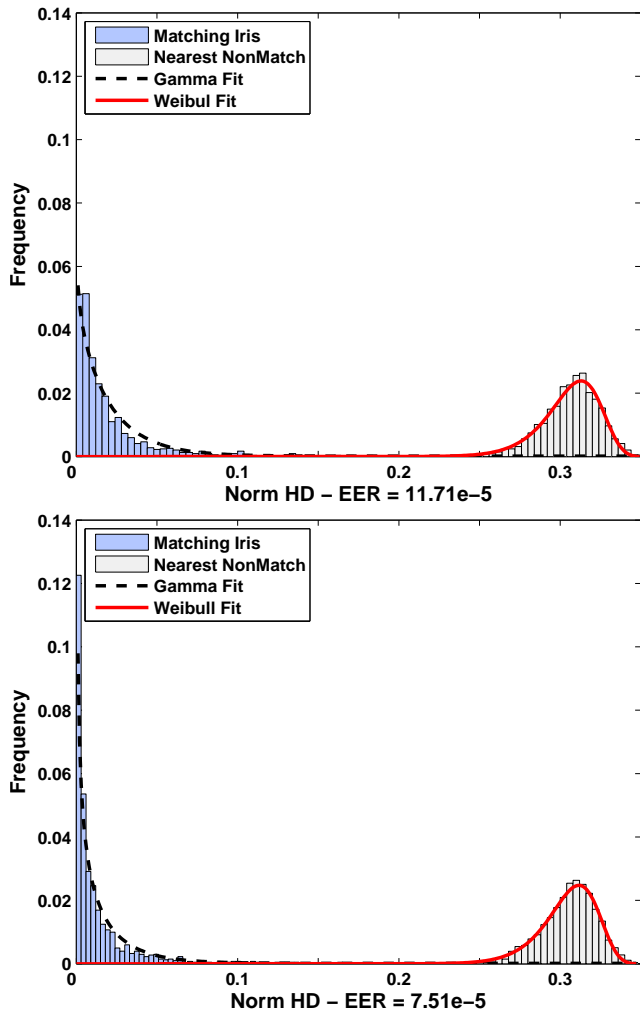


Fig. 6. Probability distributions for matching and nearest nonmatching Hamming distances for circular localization and fitting by a 3-coefficient shape description.

Fig. 6 shows the probability distributions of matching and nearest non-matching HDs for circular localization and a 3-coefficient shape description fit. Normalized for unit area, the area under the matching distribution above a chosen threshold (τ) is the False Rejection Rate (FRR), while that of the non-matching distribution below τ is the False Acceptance Rate (FAR). The Equal Error Rate (EER), which is the FAR and FRR when they are equal, is found from the area such that the integral from $-\infty$ to τ of the non-matching distribution is equal to the integral from τ to ∞ for the matching distribution. The estimated EER obtained using the proposed method was 7.51×10^{-5} ; 1.5 times lower than that obtained using circular localization (11.71×10^{-5}).

V. CONCLUSIONS

In this paper, we have described a method of modeling non-circular pupil boundaries using a Fourier-based shape description. Excellent localization results were achieved on

both general and non-ideal eye images. The use of higher numbers of Fourier coefficients to achieve better outlines was also demonstrated. The widely adopted assumption of pupil circularity was found to be unsubstantiated, with some 99.8 % of pupils falling into the non-circular category at the level of a mean error of 0.75 pixels, some with much greater error. The average error between the actual pupil boundary and the fitted outline was found to decrease significantly as the number of coefficients was increased from 1 to 9. Improvements in overall system performance in terms of EER were also observed with the proposed outline description compared to the use of circular outlines.

Future work will extend this method to model the iris boundary, which again is non circular, especially when captured off-centre. Exact pupil and iris boundary point localization remains an interesting and challenging problem, which is fundamental to the success of this or any other shape description method. Accurate pupil outline fitting is in turn an important factor in the performance of iris matching, as we have demonstrated.

ACKNOWLEDGMENT

This work was sponsored by Smart Sensors Limited, Portishead, Bristol, BS20 7BA, United Kingdom.

REFERENCES

- [1] A K. Jain, A. Ross, and S. Prabhakar, "An Introduction to Biometric Recognition," *IEEE Trans. Circuits and Systems for Video Tech.*, vol. 14, pp. 4 - 20, 2004.
- [2] P. Kronfeld, *Gross anatomy and embryology of the eye*, in: H. Davson (Ed.), *The Eye*. London: Academic Press, 1962.
- [3] J. Daugman, "High confidence visual recognition of persons by a test of statistical independence," *IEEE Trans. Pattern Analysis and Machine Intelligence*, vol. 15, pp. 1148 - 1161, 1993.
- [4] J. Daugman, "The importance of being random: Statistical principles of iris recognition," *Pattern Recognition*, vol. 36, pp. 279-291, 2003.
- [5] B. Bonney, R. Ives, D. Etter, and D. Yingzi, "Iris pattern extraction using bit planes and standard deviations," *Conf. Record of the Thirty-Eighth Asilomar Conf. on Signals, Systems and Computers*, 2004.
- [6] Y. Du, B. L. Bonney, R. W. Ives, D. M. Etter, and R. Schultz, "Analysis of Partial Iris Recognition Using a 1-D Approach", *Proc. IEEE Int'l Conf. Acoustics, Speech, and Signal Processing*, March, 2005.
- [7] "University of Bath Iris Image Database, <http://www.bath.ac.uk/elec-eng/pages/sipg/irisweb/>."
- [8] D. M. Monro, S. Rakshit and D. Zhang, DCT-based Iris Recognition, *IEEE Trans. Pattern Analysis and Machine Intelligence*, Vol. 29, No. 4, pp. 586-595, Apr 2007.